

Etherification of Functionalized Phenols with Chloroheteroarenes at Low Palladium Loading: Theoretical Assessment of the Role of Triphosphane Ligands in C–O Reductive Elimination

Mélanie Platon,^a Luchao Cui,^b Sophal Mom,^a Philippe Richard,^a Mark Saeys,^{b,*} and Jean-Cyrille Hierso^{a,*}


^a Université de Bourgogne, Institut de Chimie Moléculaire (ICMUB), UMR CNRS 5260, 9 avenue Alain Savary, 21078 Dijon, France

Fax: (+33)-3-8039-3682; e-mail: jean-cyrille.hierso@u-bourgogne.fr

^b Chemical and Pharmaceutical Engineering, Singapore – MIT Alliance, National University of Singapore, 4 Engineering Drive 3, Singapore 117576

E-mail: chesm@nus.edu.sg

Received: June 20, 2011; Revised: September 24, 2011; Published online: December 9, 2011

 Supporting information for this article is available on the WWW under <http://dx.doi.org/10.1002/adsc.201100481>.

Abstract: The present study highlights the potential of robust tridentate ferrocenylphosphanes with controlled conformation as catalytic auxiliaries in C–O bond formation reactions. Air-stable palladium triphosphane systems are efficient for selective heteroaryl ether synthesis by using as little as 0.2 mol% of catalyst. These findings represent an economically attractive and clean etherification of functionalized phenols, electron-rich, electron-poor and *para*-, *meta*- or *ortho*-substituted substrates, with heteroaryl chlorides, including pyridines, hydroxylated pyridine, pyrimidines and thiazole. The etherification tolerates very important functions in various positions, such as cyano, methoxy, amino, and fluoro groups, which is useful to synthesize bioactive molecules. DFT studies

furthermore demonstrate that triphosphane ligands open up various new pathways for the C–O reductive elimination involving the third phosphane group. In particular, the rate for one of these new pathways is calculated to be about 1000 times faster than for reductive elimination from a complex with a similar ferrocenyl ligand, but without a phosphane group on the bottom Cp-ring. Coordination of the third phosphane group to the palladium(II) center is calculated to stabilize the transition state in this new pathway, thereby enhancing the reductive elimination rate.

Keywords: C–O bond formation; mechanistic DFT study; palladium; reductive elimination; triphosphanes

Introduction

New technologies and processes for modern chemistry, such as the development of high-performance catalyst systems, have allowed progress in several key areas, such as the minimal use of declining resources. Recent investigations devoted to ligand chemistry have focused on the design, the synthesis, and the catalytic performance of polyphosphane ligands.^[1] In our group, the search for catalyst “longevity” and for lower catalyst loadings has been based on the robustness of ferrocenylphosphane ligands. This approach has afforded some success in high-value palladium-catalyzed C–C cross-couplings such as Heck, Suzuki, Sonogashira, and direct C–H activation/arylation reactions.^[1,2] Low catalyst loadings have also been ex-

plored for C–N cross-couplings, for example, in the allylic amination of achiral substrates.^[2] In addition to C–C and C–N bond formation, transition metal-catalyzed C–O bond formation has emerged as an essential synthetic tool of modern cross-coupling chemistry.^[3] Aryl and heteroaryl ethers, which are recurrent building blocks for numerous natural products,^[4] have usually been synthesized by direct nucleophilic substitution,^[5] by copper-mediated stoichiometric^[6] or catalytic reactions,^[7] by palladium-catalyzed reactions,^[8] and more recently by iron-catalyzed reactions.^[9]

In particular, palladium catalysts with monophosphane ligands displayed interesting performance for diaryl ether formation under mild conditions, and for a wide substrate scope.^[10–15] It was suggested that the efficient palladium-catalyzed etherification is driven

by the favourable influence of monophosphane ligands on the C–O reductive elimination step, and by facilitating the coupling of chloroarenes with phenols.^[11–14] In contrast, only unsatisfactory results have been reported for palladium-catalyzed aryl ether formation with diphosphane ligands, including ferrocene-based ligands.^[10] The bulkiness of the monophosphane ligands was suggested to be important for the successful coupling of demanding substrates such as electron-rich aryl chlorides and *ortho*-substituted phenols.^[14] To the best of our knowledge, only a very limited number of chloroheteroarenes have been coupled with phenol and substituted phenol derivatives. For example, Beller et al. described two examples of heteroaryl ether formation using 2.0 and 0.1 mol% of Pd/L^[12] and Buchwald et al. described three examples of heteroarene coupling with phenols using 2.0 mol% Pd/L.^[14] Hence, the development of more sustainable catalytic systems in terms of substrate-to-catalyst ratio is desirable, since typical catalyst loadings of 2 mol% or more are described for the metal-catalyzed etherification of chloroheteroarenes with demanding phenols.^[7–15] Regardless of the active transition-metal, palladium, copper or iron, lower loadings are indeed decisive to develop cleaner synthetic processes, and result in less purification steps and a reduction in solvent use and work-up. In addition, due to its price and toxicity, low catalyst loadings are now considered necessary in palladium-catalyzed reactions to further

develop large-scale industrial applications.^[12,16] In the present study, we therefore aimed to promote the coupling of a wide array of substituted heteroaryl chlorides to diversely functionalized phenols using low palladium-ligand catalyst loadings. The catalytic system we identified highlights the potential of constrained tridentate ferrocenyl polyphosphane ligands (**L7**, **L8** Figure 1) for etherification.

The influence of tridentate phosphane ligands on the C–O coupling reductive elimination step was subsequently analyzed using density functional theory (DFT-B3LYP). The calculations indicate that tridentate phosphane ligands open up various new reaction pathways in addition to the standard three-center concerted reductive elimination mechanism from square-planar bis-monodentate Pd(II) complexes. Two alternative C–O coupling reductive elimination pathways were identified in our calculations, involving the phosphane group on the bottom cyclopentadienyl (Cp) ring of the ferrocenyl ligand. This suggests that the nature of this third phosphane group will affect the C–O reductive elimination activity, in full agreement with the experimental data. The two alternative reaction pathways moreover display a lower effective activation barrier, and the careful selection of the phosphane group on the bottom Cp ring of the ferrocenyl ligand is hence expected to enhance the reductive elimination rate compared to traditional monodentate and bidentate phosphane ligands.

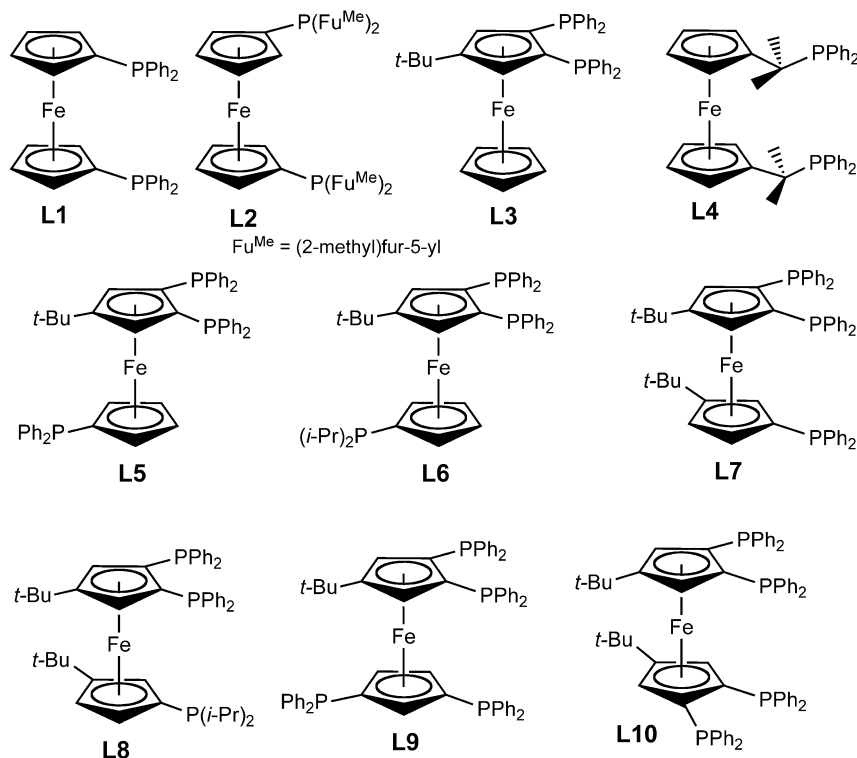


Figure 1. Di-, tri- and tetraphosphane ligand library used for C–O bond formation screening.

Results and Discussion

C–O Bond Heteroarylation Performances with Triphosphane Ligands

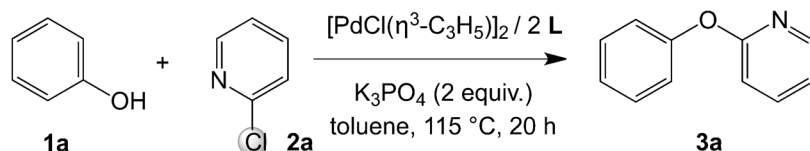
The activity of a specific set of ferrocenyl polyphosphane ligands **L1** to **L10** (Figure 1) was probed for the palladium-catalyzed arylation of phenols with chloroheteroarenes. Preliminary experiments with ferrocenyl polyphosphane ligands in the coupling of phenol to 2-chloropyridine (Table 1) indicate that using $[\text{Pd}(\eta^3\text{-allyl})(\mu\text{-Cl})_2]$ in toluene with K_3PO_4 constitutes appropriate conditions for C–O bond formation. The use of *t*-BuONa as base,^[10] THF as solvent, or $\text{Pd}(\text{OAc})_2$ ^[11] as metal source was generally less efficient. As indicated in Table 1, the performance of ferrocenyl triphosphanes (**L5–L8**, entries 5–8) is superior to either electron-rich, electron-poor or neutral ferrocenyl 1,1'-diphosphane ligands (**L4**, **L2**, **L1**, respectively, entries 4, 2 and 1), in agreement with earlier reports using B-dppf (bis-[diphenylphosphino]-ferrocene).^[10]

The decrease in the palladium chelation bite angle by using 1,2-diphosphane **L3** (entry 3) promoted undesired coupling dimerization of 2-chloropyridine. Tetraphosphanes **L9** and **L10** were found to be more efficient than diphosphanes in the heteroarylation of phenol, but, compared to triphosphanes, gave unsatisfactory results when used below 1 mol% (entries 5–10). In order to discriminate the efficiency of triphos-

phanes **L5**, **L6**, **L7** and **L8**, a catalyst loading below 0.5 mol% was necessary (entries 11–14). Under these low loadings, **L8** was found to be the best catalyst auxiliary. The ligand **L7** also displayed satisfactory performance. We therefore hypothesized that the conformation control provided by the *t*-Bu groups, a feature common to **L7** and **L8**, was related to the better performance. Having determined the optimal procedure for etherification of 2-chloropyridine at 0.2 mol% catalyst loading, the scope of this method was studied using a large variety of phenol derivatives and heteroaryl chlorides. The heteroarylation of phenol with various chloroarenes is reported in Table 2. Functionalized chloropyridine derivatives were found to be suitable substrates for coupling with phenol **1a** (entries 2 and 3). A quantitative yield of **3b** was obtained using the electron-poor 3-cyano-2-chloropyridine **2b**. For coupling of electron-rich 6-methoxy-2-chloropyridine **2c**, a higher catalyst loading of 0.5 mol% was necessary. Coupling of the chlorodiheteroarenes, 2-chloropyridazine or 2-chloropyrimidine, was also achieved quantitatively (entries 4 and 5). 2-Chloroquinoline was easily converted, and product **9** was isolated in high yield (90%, entry 6). For five-membered heterocycles the coupling of 2-thiazole was also satisfactory (entry 7).

We subsequently investigated the scope of the heteroarylation of functionalized and hindered phenol substrates with chloroheteroarenes. Under identical conditions, electron-rich functionalized phenols were

Table 1. Screening of ferrocenyl polyphosphane ligand performance in the heteroarylation of phenol **1a** with 2-chloropyridine **2a**.^[a]

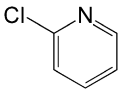
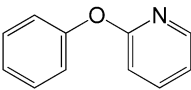
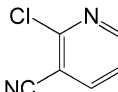
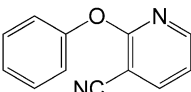
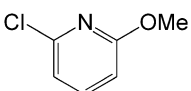
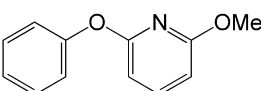
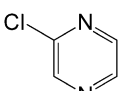
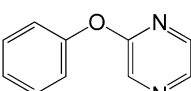
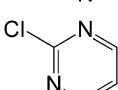
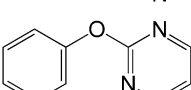
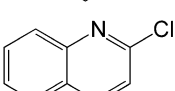
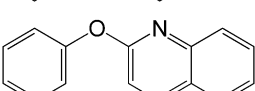
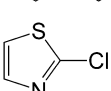
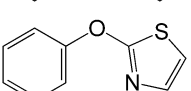


Entry	Ligand	Pd Cat. [mol%]	Conversion [%] (side product)	Yield [%] ^[b]
1	L1	1	96 (2,2'-bipyridine)	44
2	L2	1	60 (2,2'-bipyridine)	50
3	L3	1	92 (2,2'-bipyridine)	32
4	L4	1	35	35
5	L5	0.5	90	85
6	L6	0.5	100	98
7	L7	0.5	100	99
8	L8	0.5	100	99
9	L9	0.5	76	70
10	L10	0.5	80	79
11	L5	0.2	76	76
12	L6	0.2	80	73
13	L7	0.2	95	90
14	L8	0.2	100	98

^[a] $[\text{PdCl}(\eta^3\text{-C}_3\text{H}_5)]_2$:ligand **L** 1:2, phenol **1a** (2 mmol), heteroaryl chloride **2a** (2 mmol), K_3PO_4 (4 mmol), toluene 5 mL, 115 °C, 20 h under argon.

^[b] Yields of isolated products are reported.

Table 2. Heteroarylation of electron-neutral phenol **1a** with chloroheteroarenes.^[a]

Entry	Halide	Product	Pd [mol%]	Yield [%]	
1			3a	0.2	98
2			3b	0.2	99
3			3c	0.2 0.5	20 88
4			5	0.2	95
5			7	0.2	99
6			9	0.2	90
7			11	0.2	61

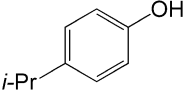
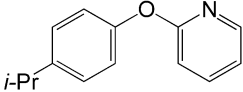
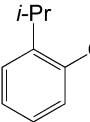
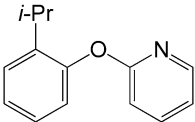
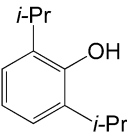
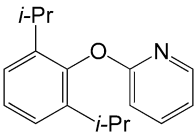
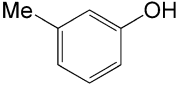
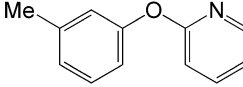
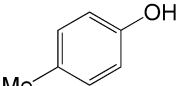
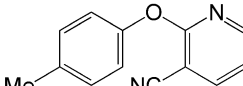
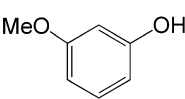
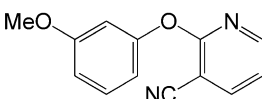
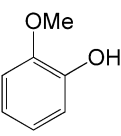
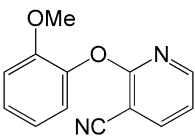
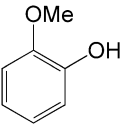
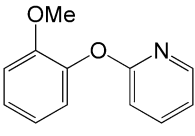
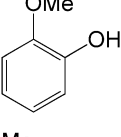
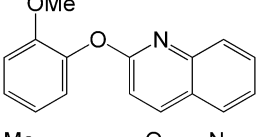
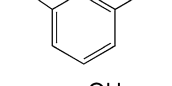
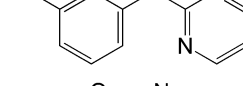
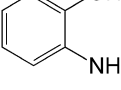
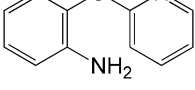
^[a] Same reaction conditions as described in Table 1, with $[\text{PdCl}(\eta^3\text{-C}_3\text{H}_5)_2]\text{:L8}$ (1:2) as the catalyst (0.004 mmol).

found to be viable substrates for palladium-catalyzed etherification of 2-chloropyridine. Good yields of products **11a** and **11b** were obtained for the coupling of phenols substituted with isopropyl groups in *para*- and *ortho*-positions (Table 3, entries 1 and 2). A steric effect is however noticeable, since 0.5 mol% of catalyst was necessary for a satisfactory yield of **11b**. The steric effect was further confirmed by the lower yield of the coupling product **11c** (55%, entry 3) obtained from the very hindered substrate **1d**. Coupling product **11d** derived from *meta*-cresol **1e** was isolated in moderate yield due to a partial decomposition during work-up (entry 4). We were glad to observe that coupling of 3-cyano-2-chloropyridine **2b** to phenols functionalized with methyl or methoxy groups in *para*-, *meta*- or *ortho*-positions produced high yields of products **12a–12c** (entries 5–7). A lower yield of 60% was obtained for the coupling of electron-rich hindered *ortho*-methoxyphenol **1h** with **2a** (entry 8).

The system also tolerates other heteroaromatic halides such as 2-chloroquinoline and 2-chloropyrimidine, since excellent yields of products **13** and **14** were obtained, even from the hindered phenol **1h** (entries 9 and 10). Finally, we were delighted to see that the coupling of the unprotected aminophenol was possible and fully selective, since product **15** was isolated in satisfactory 60% yield after work-up. Due to the

choice of the base used, no amination reaction occurred. We additionally identified some limitations in the scope of our catalyst system for the use of 3-halopyridine, which generally did not react. Under our conditions, the coupling of simple chloro- and bromoarenes with phenol was ineffective. This might open an interesting and rather unique way for selective activation of molecules incorporating both aryl and heteroaryl halides. Some other coupling reactions were efficient but the purification procedures were not satisfactory, despite repeated efforts.^[17] To further determine the scope of the Pd/L8 catalyst system, etherification for various specific substrates was conducted, as reported in Table 4. The introduction of fluorine atoms into medicinal compounds generally improves their membrane transport, general bioavailability, solubility, and metabolic stability compared to non-fluorinated analogues.^[18] Therefore we focused our attention to the heteroarylation of the fluorinated phenol **1g**. The system tolerates the presence of fluorine in the *para*-position to the hydroxy group very well. Good to high yields were obtained for the coupling products of electron-poor and electron-rich chloropyridine substrates, and, as expected, of 2-chloropyrimidine (entries 1–4). For coupling of **2c**, a catalyst loading of 0.5 mol% was necessary. We observed that the etherification tolerates very important

Table 3. Heteroarylation of functionalized and hindered electron-rich phenols with chloroheteroarenes.^[a]

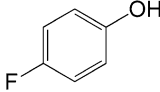
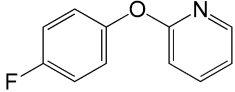
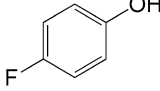
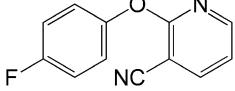
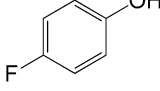
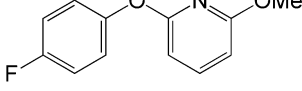
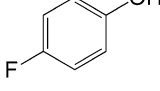
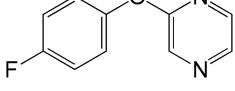
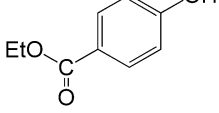
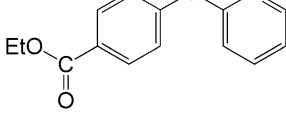
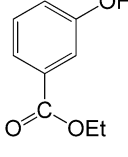
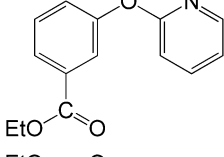
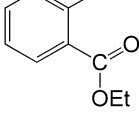
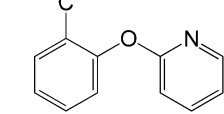
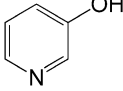
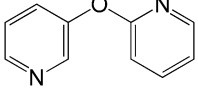
Entry	Phenol	Product	Pd [mol%]	Yield [%]
1			11a 0.2	87
2			11b 0.2	50
			0.5	75
3			11c 0.2	26
			0.5	55
4			11d 0.2	52
5			12a 0.2	92
6			12b 0.2	98
7			12c 0.2	92
8			11e 0.2	59
9			13 0.2	85
10			14 0.2	95
11			15 0.2	60

^[a] Same reaction conditions as described in Table 1, with $[\text{PdCl}(\eta^3\text{-C}_3\text{H}_5)]_2\text{:L8}$ (1:2) as the catalyst.

functions in various positions, such as cyano, methoxy, amino, and fluoro groups, which is useful to synthesize bioactive molecules. We then tested the tolerance for the presence of ester functions under our conditions. The electron-poor phenol derivatives **1i–1k** functionalized in *para*-, *meta*- and *ortho*-positions, respectively, are efficiently coupled to 2-chloropyridine with conversions above 80%. Upon work-up,

product **22** quickly decomposed on the silica column, while products **20** and **21** were isolated in good yields. Finally, with our method we report the first straightforward and clean coupling to produce 2,3-oxybis(pyridine) **23**, showing that hydroxylated pyridines are also potential candidates for diheteroaryl ether formation with chloroheteroarenes.

Table 4. Heteroarylation of fluorinated or functionalized electron-poor phenols with chloroheteroarenes.^[a]

Entry	Phenol	Product	Pd [mol%]	Yield [%]	
1		1g 	16	0.2	96
2		1g 	17	0.2	98
3		1g 	18	0.2 0.5	44 60
4		1g 	19	0.2	99
5		1i 	20	0.2	84
6		1j 	21	0.2	80
7		1k 	22	0.2	21
8		1l 	23	0.2	90

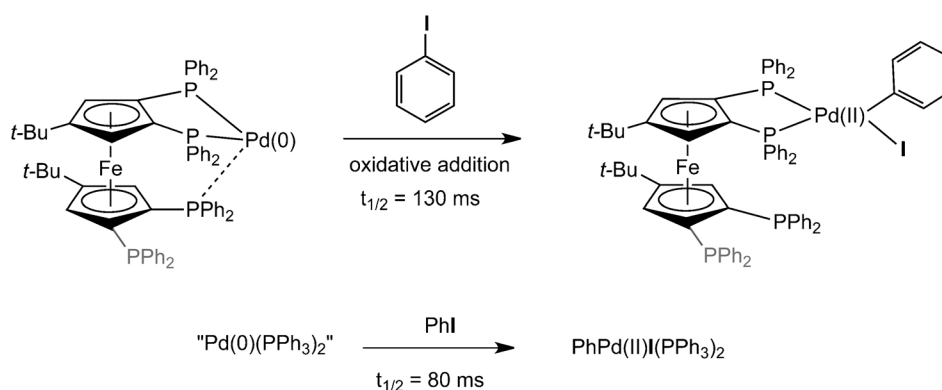
^[a] Same reaction conditions as described in Table 1, with $[\text{PdCl}(\eta^3\text{-C}_3\text{H}_5)]_2\cdot\mathbf{L8}$ (1:2) as the catalyst.

Assessment of the Influence of the Triphosphane Ligand

In order to distinguish the intrinsic efficiency of triphosphanes **L5**, **L6**, **L7** and **L8**, a palladium catalyst loading below 0.5 mol% is necessary (Table 1). It is worth noting that when using ferrocenyl triphosphane ligands, the selectivity of the reaction was remarkable, even when the conversion was only partial, since only the targeted heteroaryl ether was obtained as product. Triphosphane ligands **L5–L8** clearly possess structural features that generate a catalyst able to promote etherification which diphosphane ligands have been unable to achieve. At 0.2 mol% catalyst loading, **L7** and **L8** remain the most efficient ligands with a slight advantage for **L8**. Electrochemical studies, in combination with ³¹P NMR, on the oxidative addition of phenyl iodide to Pd(0)/**L10** complexes, which are

highly active at low loadings for Heck and Suzuki C–C bond formation,^[16b] have evidenced the influence of the third phosphorus in stabilizing the Pd(0) species before oxidative addition (Scheme 1).^[19] Therefore, the conformation of the ferrocene backbone was found to be essential in these cross-coupling reactions, with the third phosphorus atom specifically oriented towards the palladium coordination area.

Reductive elimination (R.E.) is the decisive step in aryl ether formation, and the bulkiness of electron-rich monophosphanes has been reported to promote this reaction.^[8,10,14] To elucidate the role of ferrocenyl triphosphanes in promoting the performance of palladium catalysts incorporating ligands **L5–L8**, various reductive elimination pathways were studied using DFT-B3LYP for an **L8**-stabilized Pd(II) complex with a phenoxy group and a 2-pyridinyl group. As illustrated in Figure 2, four possible reductive elimination



Scheme 1. Polyphosphane conformation stabilizing highly active Pd(0) towards oxidative addition.

pathways were identified, i.e., *via* the **RE.TS1**, the **RE.TS2**, the **RE.TS3** and the **RE.TS4** transition states.^[17] The first and fourth possible pathways involve standard direct C–O reductive elimination from a square-planar Pd(II) complex coordinated by the two phosphane groups on the top Cp-ring (**Iso.1** and **Iso.4**), with minimal involvement of the third phosphane group on the bottom Cp ring. The activation barriers are calculated to be 108 kJ mol⁻¹ and 109 kJ mol⁻¹ for pathway 1 and pathway 4, respectively, very similar to the barrier obtained when the phosphane group on the bottom Cp ring of the ferrocenyl ligand is removed, 112 kJ mol⁻¹. The product for this reductive elimination mechanism is a bidentate Pd(0) complex (**P1**), which relaxes to the more stable tridentate Pd(0) complex (**P**) without a significant barrier. Interestingly, the second and third pathway involve a Pd(II) shuttling step between the three phosphane groups, and can lead to the isomerization of the **Iso.1** and **Iso.4** complexes. Note that Pd(II) shuttling has indeed been observed experimentally, e.g., for the **L10**-Pd(II)Cl₂ complex.^[16b] Pd(II) shuttling from the phosphane groups on the top Cp ring (**Iso.1**) to a phosphane group on the top Cp ring and one on the bottom Cp ring (**Iso.2**) was calculated to be rather easy with a barrier of only 63 kJ mol⁻¹, and nearly thermoneutral. Note that the chelate bite angle in **Iso.2** is larger than that in **Iso.1** and the two Pd–P bonds are also longer (see Table A in the Supporting Information). σ -Donation from the two chelating phosphane ligands is therefore reduced in **Iso.2**, which slightly reduces the electron density at the Pd(II) center (Supporting Information, Table A). The lower electron density is expected to enhance the electron accepting capacity of the Pd(II) center, thereby facilitating C–O reductive elimination.^[20,21] Indeed, the barrier for reductive elimination from **Iso.2** is 94 kJ mol⁻¹, and 14 kJ mol⁻¹ lower than that for **Iso.1**. The effective activation barrier for C–O coupling *via* this pathway and starting from the dominant reactant species (**Iso.1**) is hence 12 kJ mol⁻¹ lower than that for

the direct pathway *via* **RE.TS1**. At 115 °C, a 12 kJ mol⁻¹ reduction in the barrier corresponds to a 40-fold increase in rate, assuming identical pre-exponential factors.

A third four-coordinated square-planar Pd(II) complex was also identified (**Iso.3**). In **Iso.3**, the Pd(II) center is coordinated by a phosphane group on the top Cp ring and the phosphane group on the bottom Cp ring. **Iso.3** is slightly less stable than **Iso.2** and can form easily from **Iso.2** with a barrier of only 23 kJ mol⁻¹. Five-coordinated Pd(II) species were calculated to be unstable for the complexes studied here. However, the distance between the Pd(II) center and the third phosphane group in **Iso.3** is only 3.34 Å, and shorter than the corresponding distances in **Iso.1** (4.06 Å) and in **Iso.2** (3.53 Å) (Supporting Information, Table A). The shorter distance to the third phosphane group increases the electron density on the Pd(II) center in **Iso.3** (Supporting Information, Table A). The increased electron density on the Pd(II) center in **Iso.3** would be expected to increase the C–O reductive elimination barrier.^[20,21] Surprisingly, the calculated barrier for reductive elimination from **Iso.3** is only 83 kJ mol⁻¹, and 25 kJ mol⁻¹ lower than the barrier for direct reductive elimination from the **Iso.1** complex. The effective activation barrier for C–O coupling *via* pathway 3 and starting from the most stable complex (**Iso.1**) is hence 19 kJ mol⁻¹ lower than that for the direct pathway *via* **RE.TS1**, which corresponds to 360-fold increase in rate at 115 °C. The role of the third phosphane group in this pathway is counterintuitive, and can be understood by analyzing the change in the Pd–P distance in going from the reactant (**Iso.3**) to the transition state (**RE.TS3**). Different from the two other pathways, the Pd(II) center approaches the third phosphane group during reductive elimination, and the distance decreases from 3.34 Å in the reactant to only 2.88 Å in the transition state, **RE.TS3** (Supporting Information, Table A). A similar decrease was not observed for the other pathways. The Pd–P distance decreases further along the

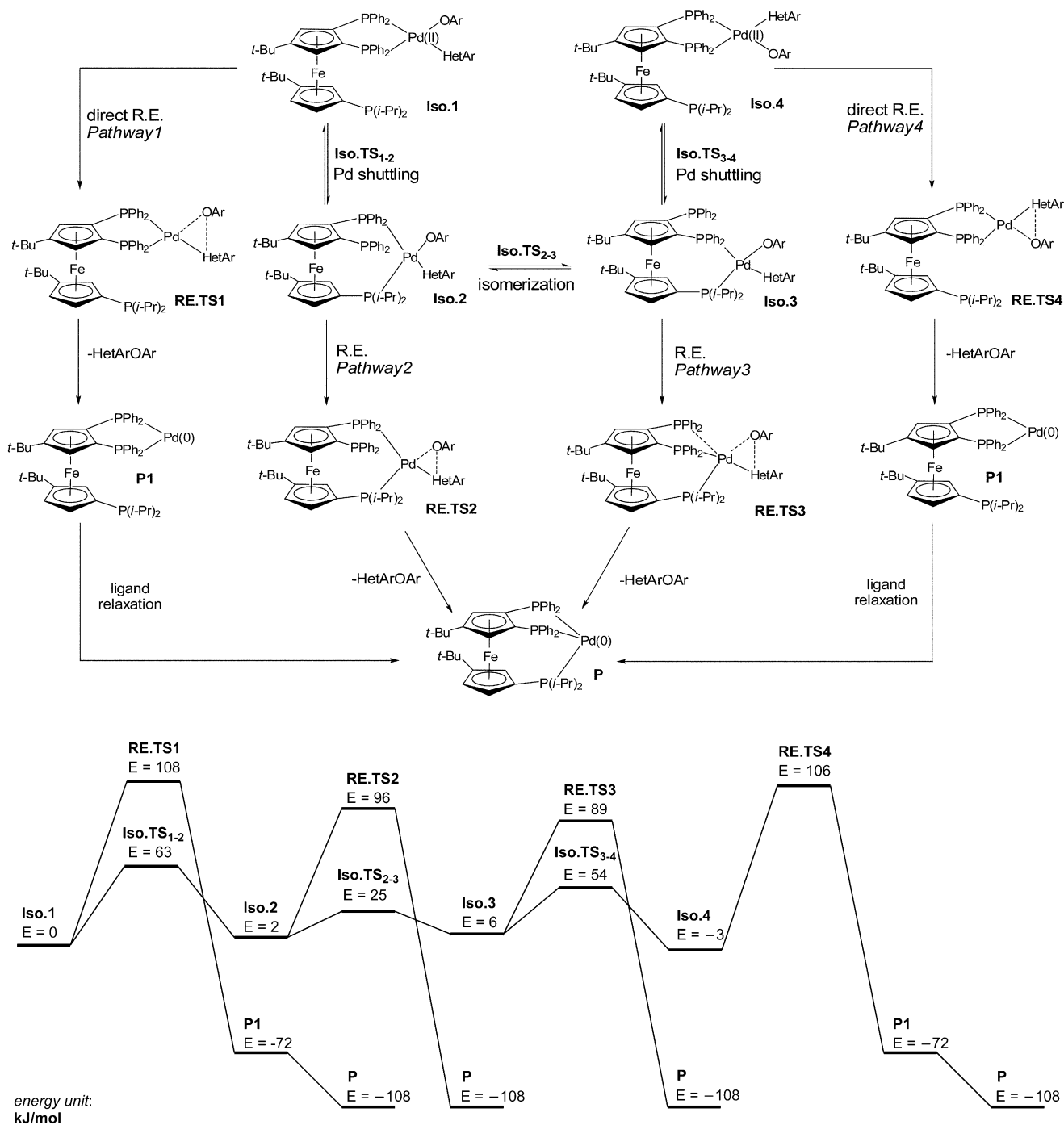
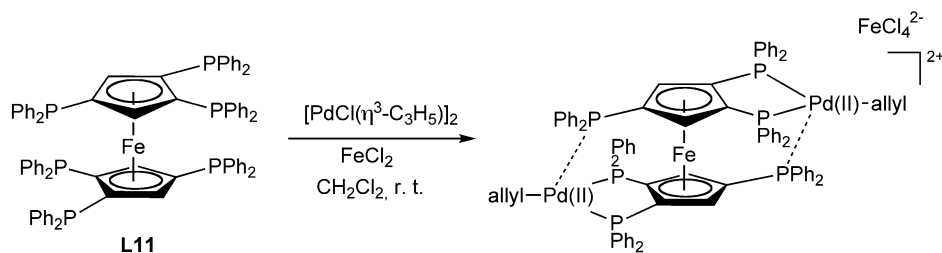


Figure 2. Proposed reaction pathways and corresponding energy profiles for reductive elimination from an **L8**-stabilized Pd(II) complex (**Iso.TS₁₋₂**, **Iso.TS₂₋₃** and **Iso.TS₃₋₄**, are shown in the Supporting Information).

reaction path, from 2.88 Å in the transition state to 2.36 Å in the tridentate Pd(0) product. *The third phosphane group therefore seems to stabilize the transition state for pathway 3, thereby enhancing the rate of C–O coupling.* This stabilization effect seems to be responsible for the low barrier for reductive elimination from **Iso.3**, despite the smaller bite angle and the higher electron-density on the Pd(II) center. Further studies are necessary to fully elucidate the electronic

origins underlying the enhanced reactivity for this novel reductive elimination pathway.

Finally, we collected conclusive experimental evidence to support the tridentate coordination modes to palladium as observed for the transition state **RE.TS3** by the DFT calculations. Despite repeated efforts, no X-ray structure has been obtained for palladium coordinated to ligands **L5–L8**. However, the synthesis of a higher rank polyphosphane,^[17] an un-



Scheme 2.

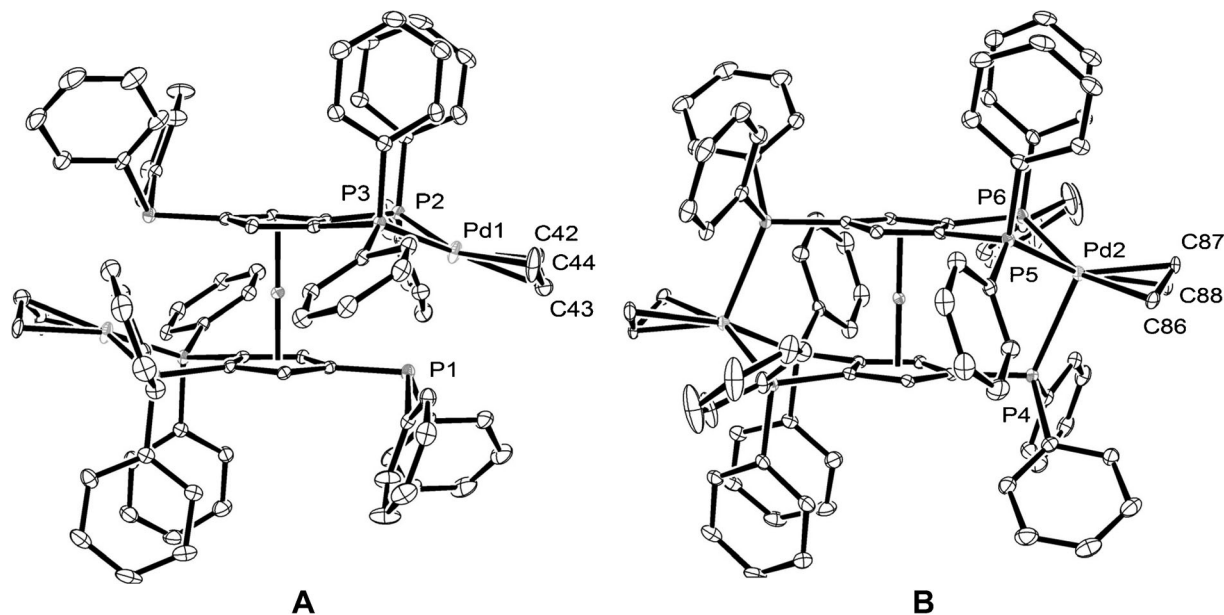


Figure 3. Molecular view of conformers **A** and **B** (thermal ellipsoids at 50% probability) of complex $[(\text{Pd}(\eta^3\text{-allyl}))_2\text{L11}][\text{FeCl}_4]$. Hydrogen atoms are omitted for clarity.

precedented hexadentate ligand **L11** with a perfect “piano-stool” conformation for two sets of three phosphanyl groups, gave us the first unambiguous proof of the labile tridentate coordination behaviour. **L11** was obtained in 65% yield by treatment of the cyclopentadienyl lithium salt $[\text{Li}][\text{Cp}(\text{PPh}_2)_3]$ with iron(II) salts. The coordination of **L11** upon treatment with $\{[\text{Pd}(\eta^3\text{-allyl})(\mu\text{-Cl})]_2\}$ in the presence of FeCl_2 , afforded the ionic bis-palladium complex $\{[\text{Pd}(\eta^3\text{-allyl})]_2\text{L11}\}[\text{FeCl}_4]$ (Scheme 2).^[22]

The coordination of bis-triphosphane **L11** to palladium(II) allylic moieties is accompanied, in addition to the expected homo-annular chelation to the palladium center, by secondary Pd–P interactions that can be of markedly different nature within the same set of crystals. The X-ray diffraction study, Figure 3, indicates that two types of closely similar coordinated edifices, **A** and **B**, coexist in the same unit cell, albeit having essential differences (Figure 4). For both conformers **A** and **B**, the two palladium coordination sites are symmetrical (C_i symmetry, see Figure 4). However, while the P–Pd distances are very similar for the chelating pairs (ranging between 2.305 and

2.349 Å), a short Pd–P distance is observed for the third phosphorus (2.618 Å) in isomer **B**, arguably indicating the presence of a bonding interaction,^[23] which does not exist in isomer **A** with a corresponding Pd⋯P interaction of 2.988 Å. This is not due to any special distortion of ligand **L11** between conformers **A** and **B**, for example the P–C_{CP} bond distances consistently ranges between 1.807 and 1.828 Å for the chelating phosphorus, and between 1.830 and 1.835 Å for P1–C_{CP} and P5–C_{CP}. To some extent the structure of conformer **B** in Figure 3 is a nice and pertinent mimic of the **RE.TS3** transition state. Consequently, these findings are convincing evidence that, even in the solid state, the conformation of the ferrocene backbone allows enough flexibility for a third phosphorus atom to interact in a labile way with a strongly P-chelated palladium(II) center.

Conclusions

We have probed the activity of a specific set of ferrocenyl polyphosphane ligands **L1** to **L10** for palladi-

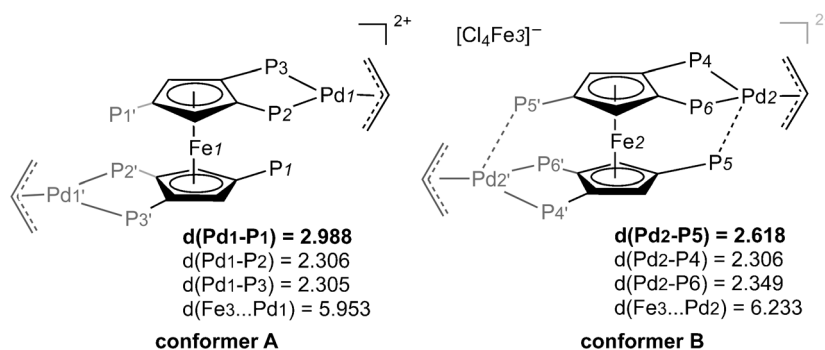


Figure 4. Solid-state bond distances (Å) and interactions in the unit cell conformers **A** and **B** of complex $[(\text{Pd}(\eta^3\text{-allyl}))_2\text{L11}][\text{FeCl}_4]$.

um-catalyzed arylation of phenols with chloroheteroarenes. As a result, we found that air-stable, moisture- and temperature-insensitive palladium/triphosphane systems are highly efficient for selective heteroaryl ether synthesis by using as little as 0.2 mol% of catalyst. In comparison with current etherification methods, the metal/ligand amount was reduced by a factor of ten to fifty. Notably, these findings represent an economically attractive and clean etherification of functionalized phenols (electron-rich, electron-poor and *para*-, *meta*- or *ortho*-substituted substrates) with heteroaryl chlorides. Most of the products prepared are potential building blocks for pharmaceuticals or agrochemicals.^[24] The present study highlights the potential of robust tridentate ferrocenylphosphanes with controlled conformation as catalytic auxiliaries in C–O bond formation reactions. DFT studies furthermore demonstrate that triphosphane ligands open up various new pathways for C–O reductive elimination involving the third phosphane group. In particular the rate for one of these new pathways is calculated to be about 1000 times faster than for reductive elimination from a complex with a similar ferrocenyl ligand, but without a phosphane group on the bottom Cp ring. Coordination of the third phosphane group to the Pd(II) center is calculated to stabilize the transition state in this new pathway, thereby enhancing the reductive elimination rate. The present catalytic results in combination with the DFT findings open the way to create new families of “multilabile” active ligands with controlled conformations,^[25] an extension of the hemilability concept.

Experimental Section

General

The reactions were carried out in oven-dried (115 °C) glassware under an argon atmosphere using Schlenk and vacuum-line techniques. The solvents were distilled over appropriate drying and deoxygenating agents prior to use. ¹H,

³¹P, ¹⁹F and ¹³C NMR, including variable-temperature NMR experiments, were performed on a 600 or 500 MHz Bruker Avance II, and a 300 MHz Bruker Avance. Electrospray exact-mass spectrometry analyses were performed on a Bruker microOTOF-Q instrument at the PACSMUB of the “Institut de Chimie Moléculaire de l’Université de Bourgogne” (ICMUB – UMR CNRS 5260). The elemental analyses were performed on a Fisons EA 1108 apparatus. GC and GC-MS analysis were done on a Supelco equity-5 capillary column on a Shimadzu GC-2014 for GC, or from an HP-5 capillary column (30 m) for GC-MS.

Catalysis

All the ferrocenyl phosphane ligands were synthesized by literature methods (see Supporting Information). The ferrocenyl ligand **L8** is available from STREM Chemicals. These phosphines are stored and weighed under air with no special precautions.

In a typical experiment, the heteroaryl chloride (2 mmol), phenol derivative (2 mmol), and K₃PO₄ (4 mmol) were introduced under argon in a Schlenk tube, equipped with a magnetic stirring bar. The $[(\text{Pd}(\eta^3\text{-allyl})(\mu\text{-Cl}))_2]/\text{ligand } \mathbf{L8}$ (ratio 1:2, 0.004 mmol Pd) catalyst and toluene (5 mL) were added, and the Schlenk tube purged several times with argon. The Schlenk tube was placed in an oil bath at 115 °C and reactants were allowed to stir for 20 h (non-optimized). Then, the reaction mixture was analyzed by gas chromatography to determine the conversion of the reagents. The solvent was removed by heating the reaction vessel under vacuum and the residue was charged directly onto a silica gel column. The products were eluted, using an appropriate eluant.

Computational Methods

C–O reductive elimination was studied using B3LYP density functional theory (DFT) as implemented in the Gaussian09 program package.^[26] The LANL2DZ basis set was used for Pd and Fe, and the 6-31G(d) basis set for the other elements. Ground state optimizations and transition state searches were performed with the Berny algorithm. Structures were confirmed to be local minima for the ground states and first-order saddle points for the transition states. Intrinsic reaction coordinate calculations connected the transition states with the correct reactant and product structures. Solvent effects were included using the SMD solvation

model with toluene as the solvent.^[27] The reported activation energies and reaction energies correspond to solvation phase electronic energy differences. Charges on the Pd center were calculated using natural population analysis (NPA).^[28]

Acknowledgements

Support provided from the CNRS (PhD grant awarded to M. P. in 3MIM program, P4-project on Heterochemistry), the ANR program for Sustainable Chemistry Development (PhD grant for S. M. from ANR-09-CP2D-03 CAMELOT), and the Région Bourgogne (PARI-SMT8), the Singapore-MIT Alliance (PhD grant for L. C.), is gratefully acknowledged. Thanks are due to R. Smaliy and V. Zinovyeva for ligand **L11** and its palladium complex preparation and characterization.

References

- [1] a) D. Laurenti, M. Feuerstein, P. Gerard, H. Doucet, M. Santelli, *J. Org. Chem.* **2001**, *66*, 1633–1637; b) J.-C. Hierso, A. Fihri, R. Amardeil, P. Meunier, H. Doucet, M. Santelli, V. V. Ivanov, *Organometallics* **2003**, *22*, 3473–3476; c) J.-C. Hierso, A. Fihri, R. Amardeil, P. Meunier, H. Doucet, M. Santelli, V. V. Ivanov, *Org. Lett.* **2004**, *6*, 3473–3476; d) V. V. Ivanov, J.-C. Hierso, R. Amardeil, P. Meunier, *Organometallics* **2006**, *25*, 989–995; e) H. Schill, A. de Meijere, D. S. Yufit, *Org. Lett.* **2007**, *9*, 2617–2620; f) S. Yu, X. Zhang, Y. Yan, C. Cai, L. Dai, X. Zhang, *Chem. Eur. J.* **2010**, *16*, 4938; g) R. V. Smaliy, M. Beaupérin, H. Cattey, P. Meunier, J.-C. Hierso, J. Roger, H. Doucet, Y. Coppel, *Organometallics* **2009**, *28*, 3152–3160; h) M. Beaupérin, A. Job, H. Cattey, S. Royer, P. Meunier, J.-C. Hierso, *Organometallics* **2010**, *29*, 2815–2822; i) J. Roger, S. Mom, M. Beaupérin, S. Royer, P. Meunier, V. V. Ivanov, H. Doucet, J.-C. Hierso, *ChemCatChem* **2010**, *2*, 296–305; j) D. Roy, S. Mom, M. Beaupérin, H. Doucet, J.-C. Hierso, *Angew. Chem. Int. Ed.* **2010**, *49*, 6650–6654; k) D. Roy, S. Mom, D. Lucas, H. Cattey, J.-C. Hierso, H. Doucet, *Chem. Eur. J.* **2011**, *17*, 6453–6461; l) V. A. Zinovyeva, C. Luo, S. Fournier, C. H. Devillers, H. Cattey, H. Doucet, J.-C. Hierso, D. Lucas, *Chem. Eur. J.* **2011**, *17*, 9901–9906.
- [2] a) A. Fihri, J.-C. Hierso, A. Vion, D. H. Nguyen, M. Urrutigoity, P. Kalck, R. Amardeil, P. Meunier, *Adv. Synth. Catal.* **2005**, *347*, 1198–1202; b) J.-C. Hierso, A. Fihri, R. Amardeil, P. Meunier, H. Doucet, M. Santelli, *Tetrahedron* **2005**, *61*, 9759–9766; c) D. H. Nguyen, M. Urrutigoity, A. Fihri, J.-C. Hierso, P. Meunier, P. Kalck, *Appl. Organomet. Chem.* **2006**, *20*, 845–850.
- [3] For recent examples of C–O bond formation, see: a) X. Wang, Y. Lu, H.-X. Dai, J.-Q. Yu, *J. Am. Chem. Soc.* **2010**, *132*, 12203–12205; b) T. J. Maimone, S. L. Buchwald, *J. Am. Chem. Soc.* **2010**, *132*, 9990–9991; c) S. Gowrisankar, A. G. Sergeev, P. Anbarasan, A. Spannenberg, H. Neumann, M. Beller, *J. Am. Chem. Soc.* **2010**, *132*, 11592–11598; d) D. Maiti, S. L. Buchwald, *J. Am. Chem. Soc.* **2009**, *131*, 17423–17429; e) D. Zhao, N. Wu, S. Zhang, P. Xi, X. Su, J. Lan, J. You, *Angew. Chem.* **2009**, *121*, 8885–8888; *Angew. Chem. Int. Ed.* **2009**, *48*, 8729–8732; f) A. A. Alonso, C. Nájera, I. M. Pastor, M. Yus, *Chem. Eur. J.* **2010**, *16*, 5274–5284.
- [4] For examples of biologically active heteroaryl ethers, see: a) J. J. Kennedy-Smith, N. Arora, J. R. Billedeau, J. Fretland, J. Q. Hang, G. M. Heilek, S. F. Harris, D. Hirschfeld, H. Javanbakht, Y. Li, W. Liang, R. Roetz, M. Smith, G. Su, J. M. Suh, A. G. Villaseñor, J. Wu, D. Yasuda, K. Klumppd, Z. K. Sweeney, *Med. Chem. Commun.* **2010**, *1*, 79–83; b) S. K. Tipparaju, S. P. Muench, E. J. Mui, S. N. Ruzheinikov, J. Z. Lu, S. L. Hutson, M. J. Kirisits, S. T. Prigge, C. W. Roberts, F. L. Henriquez, A. P. Kozikowski, D. W. Rice, R. L. McLeod, *J. Med. Chem.* **2010**, *53*, 6287–6300; c) D.-S. Su, J. J. Lim, E. Tinney, T. J. Tucker, S. Saggari, J. T. Sisko, B.-L. Wana, M. B. Young, K. D. Anderson, D. Rudd, V. Munshi, C. Bahnck, P. J. Felock, M. Lu, M.-T. Lai, S. Touch, G. Moyer, D. J. DiStefano, J. A. Flynn, Y. Liang, R. Sanchez, R. Perlow-Poehnel, M. Miller, J. P. Vacca, T. M. Williams, N. J. Anthony, *Bioorg. Med. Chem. Lett.* **2010**, *20*, 4328–4332; d) K. Nakamoto, I. Tsukada, K. Tanaka, M. Matsukura, T. Haneda, Satoshi Inoue, N. Murai, S. Abe, N. Ueda, M. Miyazaki, N. Watanabe, M. Asada, K. Yoshimatsu, K. Hata, *Bioorg. Med. Chem. Lett.* **2010**, *20*, 4624–4626; e) R. P. Wurz, L. H. Pettus, B. Henkle, L. Sherman, M. Plant, K. Miner, H. J. McBride, L. M. Wong, C. J. M. Saris, M. R. Lee, S. Chmait, C. Mohr, F. Hsieh, A. S. Tasker, *Bioorg. Med. Chem. Lett.* **2010**, *20*, 1680–1684.
- [5] For examples, see: a) Y.-J. Cherng, *Tetrahedron* **2002**, *58*, 887–890; b) M. Lloung, A. Loupy, S. Marque, A. Petit, *Heterocycles* **2004**, *63*, 297–308.
- [6] a) F. Ullmann, *Ber. Dtsch. Chem. Ges.* **1904**, *37*, 853–854. For scaled-up applications, see: b) J. W. H. Watthey, M. Desai, *J. Org. Chem.* **1982**, *47*, 1755–1759; c) S. Caron, N. M. Do, J. E. Sieser, D. C. Whritenour, P. D. Hill, *Org. Process Res. Dev.* **2009**, *13*, 324–330. Developments of Ullmann coupling employed sub-stoichiometric amount of copper (30 to 50 mol%), see: d) Q. Cai, B. Zou, D. Ma, *Angew. Chem.* **2006**, *118*, 1298–1301; *Angew. Chem. Int. Ed.* **2006**, *45*, 1276–1279; e) Y. Zhao, Y. Wang, H. Sun, L. Li, H. Zhang, *Chem. Commun.* **2007**, 3186–3187.
- [7] Copper-catalyzed leading methodologies for heteroaryl ethers formation employed heteroaryl bromides in the presence of 10 to 15 mol% copper halide with 20 to 40 mol% ligand, see: a) D. Maiti, S. L. Buchwald, *J. Org. Chem.* **2010**, *75*, 1791–1794; b) Q. Zhang, D. Wang, X. Wang, K. Ding, *J. Org. Chem.* **2009**, *74*, 7187–7190; c) N. D. D'Angelo, J. J. Peterson, S. K. Booker, I. Fellows, C. Dominguez, R. Hungate, P. J. Reider, T.-S. Kim, *Tetrahedron Lett.* **2006**, *47*, 5045–5048; d) B. H. Lipshutz, J. B. Unger, B. R. Taft, *Org. Lett.* **2007**, *9*, 1089–1092; e) R. A. Altman, S. L. Buchwald, *Org. Lett.* **2007**, *9*, 643–646.
- [8] For seminal works, see: a) M. Palucki, J. P. Wolfe, S. L. Buchwald, *J. Am. Chem. Soc.* **1996**, *118*, 10333–10334; b) G. Mann, J. F. Hartwig, *J. Am. Chem. Soc.* **1996**, *118*, 13109–13110.

- [9] a) N. Xia, M. Taillefer, *Chem. Eur. J.* **2008**, *14*, 6037–6039; b) O. Bistri, A. Correa, C. Bolm, *Angew. Chem.* **2008**, *120*, 596–598; *Angew. Chem. Int. Ed.* **2008**, *47*, 586–588.
- [10] a) G. Mann, C. Incarvito, A. R. L. Rheingold, J. F. Hartwig, *J. Am. Chem. Soc.* **1999**, *121*, 3224–3225; b) R. A. Widenhoefer, S. L. Buchwald, *J. Am. Chem. Soc.* **1998**, *120*, 6504–6511.
- [11] A. Aranyos, D. W. Old, A. Kiyomori, J. P. Wolfe, J. P. Sadighi, S. L. Buchwald, *J. Am. Chem. Soc.* **1999**, *121*, 4369–4378.
- [12] S. Harkal, K. Kumar, D. Michalik, A. Zapf, R. Jackstell, F. Rataboul, T. Riermeir, A. Monsees, M. Beller, *Tetrahedron Lett.* **2005**, *46*, 3237–3240.
- [13] M. A. Fernández-Rodríguez, Q. Shen, J. F. Hartwig, *Chem. Eur. J.* **2006**, *12*, 7782–7796.
- [14] C. H. Burgos, T. E. Barder, X. Huang, S. L. Buchwald, *Angew. Chem.* **2006**, *118*, 4427–4432; *Angew. Chem. Int. Ed.* **2006**, *45*, 4321–4326.
- [15] T. Hu, T. Schulz, C. Torborg, X. Chen, J. Wang, M. Beller, J. Huang, *Chem. Commun.* **2009**, 7330–7332. In this most recent work two *ortho*-substituted aryl chlorides are coupled by using 6 mol% of monophosphane ligand and 2 mol% of palladium.
- [16] a) V. Farina, *Adv. Synth. Catal.* **2004**, *346*, 1553–1582; b) J.-C. Hierso, M. Beaupérin, P. Meunier, *Eur. J. Inorg. Chem.* **2007**, 3767–3780.
- [17] See Supporting Information for details.
- [18] P. Anbarasan, H. Neumann, M. Beller, *Chem. Asian J.* **2010**, *5*, 1775–1778.
- [19] D. Evrard, D. Lucas, Y. Mugnier, P. Meunier, J.-C. Hierso, *Organometallics* **2008**, *27*, 2643–2653.
- [20] L. Cui, M. Saeys, *ChemCatChem* **2011**, *3*, 1060–1064.
- [21] J. F. Hartwig, *Organotransition Metal Chemistry: From Bonding to Catalysis*, University Science Books, Sausalito, **2010**, pp 322.
- [22] Single crystals suitable for X-ray precipitated in high yield, in less than 24 h, at room temperature from dichloromethane. The corresponding crystal structure has been deposited at the CCDC and allocated the deposition number CCDC 812731. These data can be obtained free of charge from The Cambridge Crystallographic Data Centre via www.ccdc.cam.ac.uk/data_request/cif.
- [23] The existence of a strong interaction here is unquestionable, but X-ray characterization of unambiguous long Pd⋯P bonding involving a clear lone-pair donation are rare and have been found between 2.50 and 2.65 Å, see for instance, from a CSD search (10/2010): a) X. Sava, L. Ricard, F. Mathey, P. Le Floch, *Chem. Eur. J.* **2001**, *7*, 3159, [Pd⋯P=2.6076(8) Å]; b) S.-I. Aizawa, T. Iida, Y. Sone, T. Kawamoto, S. Funahashi, S. Yamada, M. Nakamura, *Bull. Chem. Soc. Jpn.* **2002**, *75*, 91, [Pd⋯P=2.637(18) Å]; c) J. R. Martinelli, D. A. Watson, D. M. M. Freckmann, T. E. Barder, S. L. Buchwald, *J. Org. Chem.* **2008**, *73*, 7102, [Pd⋯P=2.5075(8) Å]; d) T. Mizuta, C. Miyaji, T. Katayama, J. Ushio, K. Kubo, K. Miyoshi, *Organometallics* **2009**, *28*, 539, [Pd⋯P=2.5031(13) Å].
- [24] For a selection of examples, see: a) T. Glinka, O. Rodny, K. A. Bostian, D. M. Wallace, R. I. Higuchi, C. Chow, C. C. Mak, G. Hirst, B. Eastman, *U. S. Pat. Appl. Publ.* 20100152098A1 20100617, **2010**; b) T. Oe, Y. Ono, K. Kawasaki, T. Nakajima, *Eur. Pat. Appl.* 359547A1 19900321, **1990**; c) J. M. Clough, C. R. A. Godfrey, S. P. Heaney, K. Anderton, *Eur. Pat. Appl.* 312243A2 19890419, **1989**; d) A. J. Hill, J. W. McGraw *J. Org. Chem.* **1949**, *14*, 783; e) A. Serban; K. G. Watson, R. B. Warner, *Pat. Specif. Aust.* AU 535637 B2 19840329, **1984**.
- [25] The term “multilability” could be coined as an extension of “hemilability” for polydentate ligands having more than two donor groups, therein of the same nature. For a definition and review of “hemilability”, see: P. Braunstein, F. Naud, *Angew. Chem.* **2001**, *113*, 702–722; *Angew. Chem. Int. Ed.* **2001**, *40*, 680–699.
- [26] M. J. Frisch, G. W. Trucks, H. B. Schlegel, G. E. Scuseria, M. A. Robb, J. R. Cheeseman, G. Scalmani, V. Barone, B. Mennucci, G. A. Petersson, H. Nakatsuji, M. Caricato, X. Li, H. P. Hratchian, A. F. Izmaylov, J. Bloino, G. Zheng, J. L. Sonnenberg, M. Hada, M. Ehara, K. Toyota, R. Fukuda, J. Hasegawa, M. Ishida, T. Nakajima, Y. Honda, O. Kitao, H. Nakai, T. Vreven, J. A. Montgomery, Jr., J. E. Peralta, F. Ogliaro, M. Bearpark, J. J. Heyd, E. Brothers, K. N. Kudin, V. N. Staroverov, R. Kobayashi, J. Normand, K. Raghavachari, A. Rendell, J. C. Burant, S. S. Iyengar, J. Tomasi, M. Cossi, N. Rega, J. M. Millam, M. Klene, J. E. Knox, J. B. Cross, V. Bakken, C. Adamo, J. Jaramillo, R. Gomperts, R. E. Stratmann, O. Yazyev, A. J. Austin, R. Cammi, C. Pomelli, J. W. Ochterski, R. L. Martin, K. Morokuma, V. G. Zakrzewski, G. A. Voth, P. Salvador, J. J. Dannenberg, S. Dapprich, A. D. Daniels, Ö. Farkas, J. B. Foresman, J. V. Ortiz, J. Cioslowski, D. J. Fox, *Gaussian 09, Revision A.02*, Gaussian, Inc., Wallingford, CT, **2009**.
- [27] A. V. Marenich, C. J. Cramer, D. G. Truhlar, *J. Phys. Chem. B* **2009**, *113*, 6378–6396.
- [28] A. E. Reed, R. B. Weinstock, F. Weinhold, *J. Chem. Phys.* **1985**, *83*, 735–746.